ELSEVIER

Thermochimica Acta 250 (1995) 151-163

thermochimica
acta

The preparation and thermal decomposition of some metal compounds of 4-dimethylaminobenzylidenepyruvate in the solid state

D.E. Rasera, L.C.S. Oliveira, C.B. Melios, M. Ionashiro *

Instituto de Química, Universidade Estadual Paulista, Araraquara, C.P. 355, São Paulo, CEP. 14.800-900, Brazil

Received 13 December 1993; accepted 11 July 1994

Abstract

Solid M-DMBP compounds, where M represents Mg(II), Ca(II), Sr(II), Ba(II), Ni(II), Cu(II), Zn(II), Fe(III), La(III), Th(IV), and DMBP is 4-dimethylaminobenzylidenepyruvate, have been prepared. Thermogravimetry–derivative thermogravimetry (TG–DTG), differential scanning calorimetry (DSC) and other methods of analysis have been used to characterize and to study the thermal stability and thermal decomposition of these compounds.

Keywords: Decomposition; DSC; DTG; Stability; TG; XRD

1. Introduction

The preparation and investigation of several metal-ion complexes with DMBP $(CH_3)_2$–N––CH=CH–CO–COO–, have been studied in aqueous solutions [1–3]. Solid state compounds of lanthanide(III) and yttrium(III) with DMBP have previously been prepared and studied using TG–DTG, DSC and X-ray powder diffractometry [4]. No reference has been found concerning the preparation of other solid-state metal–DMBP compounds.

In this study, solid state compounds of Mg(II), Ca(II), Sr(II), Ba(II), Ni(II), Cu(II), Zn(II), Fe(III), La(III), Th(IV) with DMBP were prepared. These com-

---

* Corresponding author.

SSDI 0040-6031(94)01987-8

Table 1
Analytical and thermoanalytical TG [a] results

Compound	Metal in %			DMBP [b] in %		Water in %	
	Theor.	TG	EDTA	Theor.	TG	Theor.	TG
$Mg(DMBP)_2 \cdot 2H_2O$	4.89	5.02	4.31	84.64	84.27	7.25	7.41
$Ca(DMBP)_2 \cdot 3.5H_2O$	7.43	7.64	7.15	77.92	77.61	11.69	11.70
$Sr(DMBP)_2 \cdot 1.5H_2O$	15.90	15.85	16.38	76.29	76.73	4.91	4.52
$Ba(DMBP)_2 \cdot H_2O$	23.20	23.57	22.80	63.62	63.11	3.04	3.03
$Ni(DMBP)_2 \cdot 2.5H_2O$	10.87	10.58	10.69	77.83	78.69	8.34	7.84
$Cu(DMBP)_2 \cdot 0.5H_2O$	12.48	12.06	11.88	85.75	86.44	1.77	1.50
$Zn(DMBP)_2 \cdot H_2O$	12.57	12.90	12.12	80.88	80.41	3.47	3.54
$Fe(DMBP)_3 \cdot H_2O$	7.67	7.35	6.84	86.57	87.21	2.47	2.28
$La(DMBP)_3 \cdot 2H_2O$	16.74	16.36	15.93	76.02	76.72	4.35	4.51
$Th(DMBP)_4 \cdot 2H_2O$	20.33	20.87	20.11	73.70	73.12	3.16	3.13

[a] TG in platinum crucible. [b] DMBP is 4-dimethylaminobenzylidenepyruvate.

pounds were characterized and studied by complexometric titration, TG–DTG, DSC and X-ray powder diffractometry. The data obtained allowed us to acquire new information concerning these compounds in the solid state, including their thermal stability and thermal decomposition.

2. Experimental

DMBP was prepared as previously described [1]. The solid state compounds were prepared by mixing solutions of the corresponding metal chlorides with a solution of DMBP, until total precipitation of the metal ions. For Fe(III) and Th(IV), due to the acidity of the respective solutions and to avoid the decomposition of the DMBP, the solid state compounds were prepared by mixing a solution of DMBP with a solution of the corresponding metal chloride and nitrate, respectively, also until total precipitation. The precipitates were washed, filtered, dried and stored as previously described [4].

In the solid state compounds, DMBP was determined from the TG–DTG curves, and the metal ions were determined from the TG–DTG curves and by complexometric titrations with standard EDTA solutions; Mg(II), Ca(II), Sr(II), Ba(II), Fe(III) [5]; Ni(II), Cu(II), Zn(II) [6]; La(III) [7] and Th(IV) [8].

The TG–DTG and DSC curves were obtained using a Mettler TA-4000 thermoanalyser system with an air flux of ≈ 150 ml min^{-1}, a heating rate of 5°C min^{-1} and with samples weighing about 7 mg [9].

Diffraction patterns were obtained with an HGZ 4/B horizontal diffractometer (Germany) equipped with a proportional counter and pulse height discriminator [10].

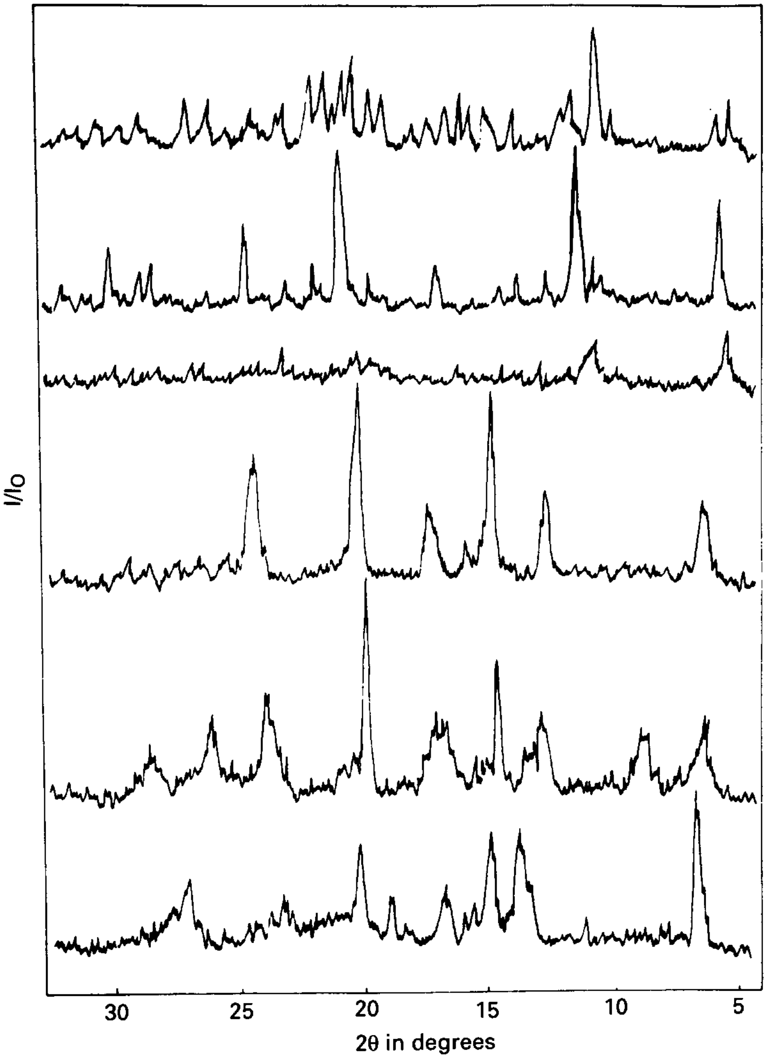

Fig. 1. X-ray powder diffraction patterns (from top to bottom) $Mg(DMBP)_2 \cdot 2H_2O$, $Ca(DMBP)_2 \cdot 3.5H_2O$; $Sr(DMBP)_2 \cdot 1.5H_2O$, $Ni(DMBP)_2 \cdot 2.5H_2O$, $Cu(DMBP)_2 \cdot 0.5H_2O$ and $Zn(DMBP)_2 \cdot H_2O$.

3. Results and discussion

Table 1 presents the analytical and thermoanalytical (TG) data for the prepared compounds from which the general formula $M^{m+}(DMBP)_m \cdot nH_2O$ can be established, where M represents metals, DMBP is 4-dimethylaminobenzylidenepyruvate, $m = 2-4$ and $n = 0.5-3.5$.

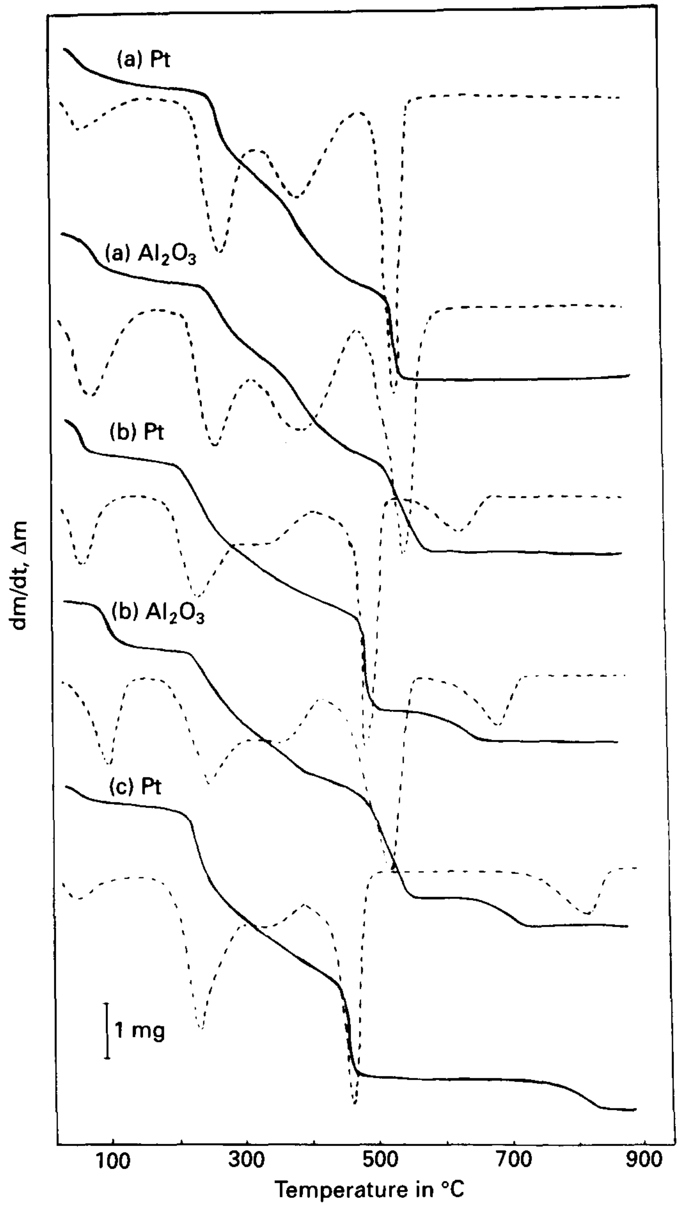

Fig. 2. TG-DTG curves of the compounds: (a) $Mg(DMBP)_2 \cdot 2H_2O$ (Pt, 7.393 mg; Al_2O_3, 7.380 mg); (b) $Ca(DMBP)_2 \cdot 3.5H_2O$ (Pt, 7.511 mg; Al_2O_3, 7.594 mg); (c) $Sr(DMBP)_2 \cdot 1.5H_2O$ (Pt, 7.723 mg; Al_2O_3, 7.352) mg); (d) $Ba(DMBP)_2 \cdot H_2O$ (Pt, 7.799 mg; Al_2O_3, 7.444 mg); (e) $Ni(DMBP)_2 \cdot 2.5H_2O$ (Pt, 7.692 mg; Al_2O_3, 7.502 mg); (f) $Cu(DMBP)_2 \cdot 0.5H_2O$ (Pt, 7.278 mg; Al_2O_3, 7.475 mg); (g) $Zn(DMBP)_2 \cdot H_2O$ (Pt, 7.264 mg; Al_2O_3, 7.189 mg); (h) $Fe(DMBP)_3 \cdot H_2O$ (Pt, 7.278 mg; Al_2O_3, 7.475 mg); (i) $La(DMBP)_3 \cdot 2H_2O$ (Pt, 7.930 mg; Al_2O_3, 7.635 mg); and (j) $Th(DMBP)_4 \cdot 2H_2O$ (Pt, 7.382 mg; Al_2O_3, 7.679 mg).

The X-ray powder patterns, Fig. 1, show that the more soluble magnesium, calcium, strontium, nickel, copper and zinc compounds tend towards a crystalline structure. The diffraction patterns for the barium, iron, lanthanum and thorium compounds, which are less soluble, indicate an amorphous structure. The crystallinity is undoubtedly related to the solubility of these compounds.

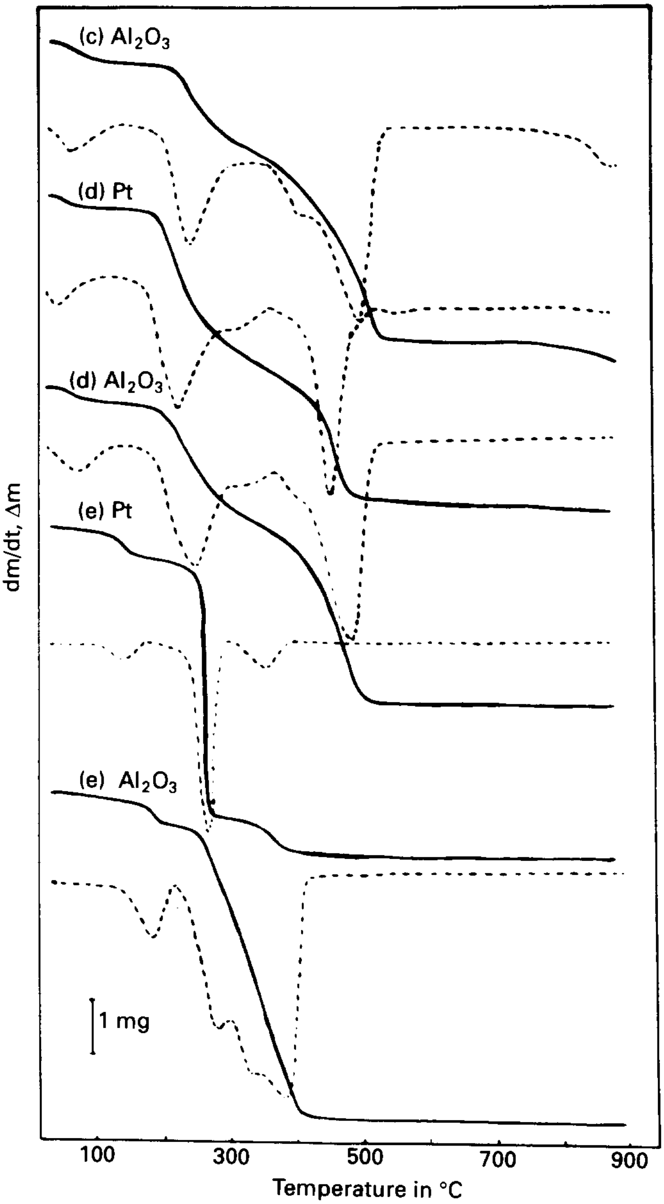

Fig. 2 (continued).

The TG–DTG curves obtained in a platinum crucible and in an alumina crucible with a perforated cover are shown in Fig. 2. The TG curves show mass losses in steps which depend on the metal present. In an alumina sample holder with a perforated cover, the thermal decomposition of the anhydrous compounds was

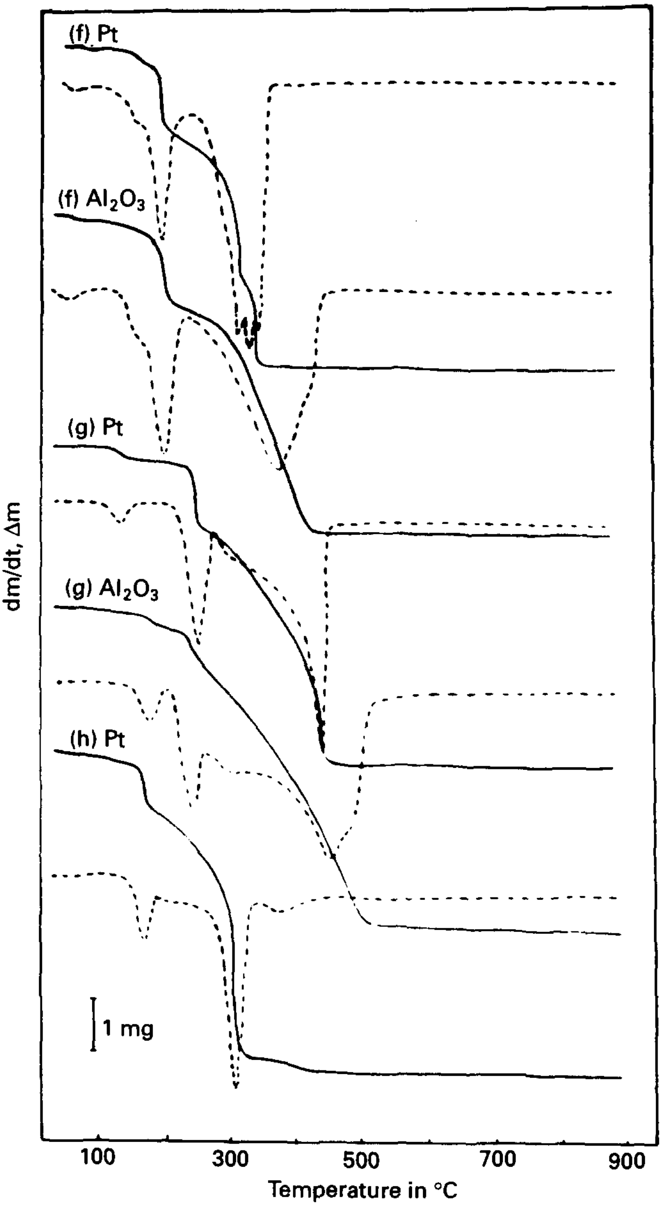

Fig. 2 (continued).

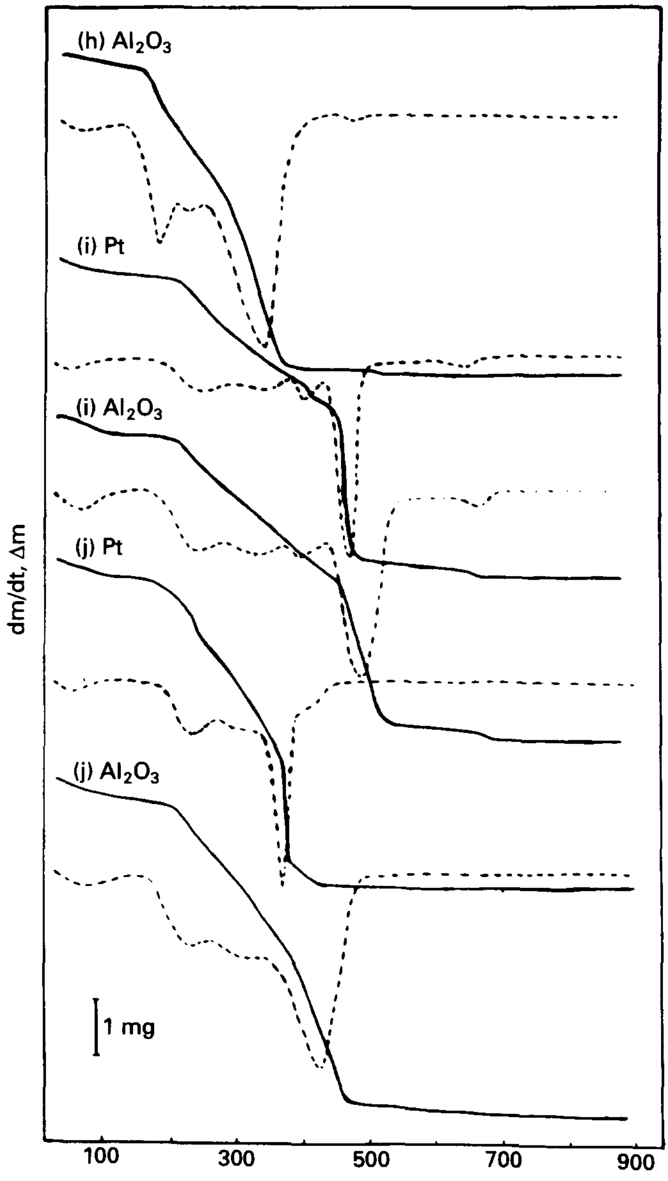

Fig. 2 (continued).

much less rapid than in a platinum crucible for the iron, nickel, copper and thorium compounds. However, for the alkaline earths (except beryllium and radium) and lanthanum compounds, no significant difference was observed.

For the anhydrous compounds, except for Zn(II) and Fe(III) in the Pt crucible and Mg(II) in both crucibles, the DTG curves show that the thermal decomposi-

Table 2
Mass loss m and temperature range corresponding to the partial thermal decomposition of the compounds $M(DMBP)_m \cdot nH_2O$, where M represents metals, DMBP is 4-dimethylaminobenzylidenepyruvate, $m = 2$–4 and $n = 0.5$–3.5

m in mg	θ in °C	Partial thermal decomposition	Loss in %	
			Theor.	Exp.
$Mg(DMBP)_2$ [a]				
0.546	30–135	$2H_2O$	7.25	7.41
1.296	187–275	$2(CH_3)_2$–N	17.74	17.59
2.675	275–440	2(⌬); CH=CH	35.91	36.30
2.241	440–550	Rest of the ligand with formation of MgO	31.01	30.41
$Mg(DMBP)_2$ [b]				
0.546	30–150	$2H_2O$	7.25	7.40
1.334	200–302	$2(CH_3)_3$–N	17.74	18.08
2.636	302–475	2(⌬); CH=CH	35.91	35.72
2.217	475–586	Rest of the ligand with formation of MgO	31.01	30.04
$Ca(DMBP)_2$ [a]				
0.879	30–100	$3.5H_2O$	11.69	11.70
3.306	100–480	$2(CH_3)_2$–N–⌬	44.54	44.02
1.921	480–500	Rest of the ligand with formation of $CaCO_3$	25.22	25.57
0.602	400–650	CO_2, with formation of CaO	8.16	8.01
$Ca(DMBP)_2$ [b]				
0.912	30–125	$3.5H_2O$	11.69	12.01
3.316	125–490	$2(CH_3)_2$–N–⌬	44.54	43.66
1.958	490–550	Rest of the ligand with formation of $CaCO_3$	25.22	25.78
0.595	550–710	CO_2, with formation of CaO	8.16	7.84
Sr $(DMBP)_2$ [a]				
0.349	30–132	$1.5H_2O$	4.91	4.52
3.369	132–438	$2(CH_3)_2$–N–⌬	43.61	43.62
1.950	438–489	Rest of the ligand with formation of $SrCO_3$	24.69	25.25
0.607	489–850	CO_2, with formation of SrO	7.99	7.86
Sr(DMBP) [b]				
0.365	30–150	$1.5H_2O$	4.91	4.96
1.196	150–285	$2(CH_3)_2$–N	16.00	16.27
3.813	285–535	Rest of the ligand with formation of $SrCO_3$	52.31	51.86
	750–900	Partial thermal decomposition of $SrCO_3$		
$Ba(DMBP)_2$ [a]				
0.236	30–120	$1H_2O$	3.04	3.03
3.137	120–421	$2(CH_3)_2$–N–⌬	40.62	40.22
1.785	421–523	Rest of the ligand with formation of $BaCO_3$	23.00	22.89
$Ba(DMBP)_2$ [b]				
0.238	30–125	$1H_2O$	3.04	3.20
2.097	125–375	$2(CH_3)_2$–N; ⌬	27.75	27.66
2.369	375–550	Rest of the ligand with formation of $BaCO_3$	35.87	35.45
$Ni(DMBP)_2$ [a]				
0.603	30–200	$2.5H_2O$	8.33	7.84
5.343	200–281	Pyrolysis of the ligand with formation of NiO_3	69.69	69.46
0.681	281–400	CO_2, with formation of NiO	8.15	8.85

Table 2 (continued)

m in mg	θ in °C	Partial thermal decomposition	Loss in %	
			Theor.	Exp.
Ni(DMBP)$_2$ [b]				
0.598	30–220	2.5H_2O	8.33	7.97
5.829	220–430	Pyrolysis of the ligand, with formation of NiO	77.83	77.70
Cu(DMBP)$_2$ [a]				
0.110	30–100	0.5H_2O	1.77	1.50
0.400	120–188	2CH_3	5.91	5.46
0.788	188–196	2CH_3–N	11.41	10.75
2.238	196–318	2 ⌬	29.90	30.52
2.896	318–420	Rest of the ligand, with formation of CuO	38.53	39.49
Cu(DMBP)$_2$ [b]				
0.129	30–100	0.5H_2O	1.77	1.68
1.302	130–206	2$(CH_3)_2$–N	17.32	16.96
5.316	206–450	Rest of the ligand, with formation of CuO	68.43	69.24
Zn(DMBP)$_2$ [a]				
0.257	50–175	1H_2O	3.47	3.54
1.191	175–260	2$(CH_3)_2$–N	16.56	16.40
0.681	260–525	Rest of the ligand, with formation of ZnO	63.92	64.01
Zn(DMBP)$_2$ [b]				
0.267	50–185	1H_2O	3.47	3.71
0.625	185–247	3CH_3	8.68	8.69
5.428	247–725	Rest of the ligand, with formation of ZnO	75.28	75.50
Fe(DMBP)$_3$ [a]				
0.166	30–130	1H_2O	2.47	2.28
0.902	130–175	3$(CH_3)_2$	12.38	12.39
5.162	175–325	Rest of the ligand with formation of $Fe_2O_2CO_3$	71.16	70.93
0.283	325–430	0.5CO_2, with formation of Fe_2O_3	3.02	3.89
Fe(DMBP)$_3$ [b]				
0.188	30–130	1H_2O	2.47	2.52
1.243	130–208	2CH_3; 2$(CH_3)_2$–N	16.23	16.63
1.701	208–292	N–⌬; ⌬	22.81	22.76
3.552	292–500	Rest in the ligand, with formation of Fe_2O_3	47.53	47.52
La(DMBP)$_3$ [a]				
0.358	30–125	2H_2O	4.34	4.51
2.718	150–440	3$(CH_3)_2$N; 2(⌬)	34.28	34.27
2.845	440–535	Rest of the ligand with formation of $La_2O(CO_3)_2$	36.43	35.88
0.366	535–700	1CO_2, with formation of La_2O_3	5.30	4.62
La(DMBP)$_3$ [b]				
0.320	30–150	2H_2O	4.34	4.19
2.632	174–450	3$(CH_3)_2$–N; 2(⌬)	34.28	34.47
2.791	450–549	Rest of the ligand with formation of $La_2O(CO_3)_2$	36.43	36.56
0.441	549–740	1CO_2, with formation of La_2O_3	5.30	5.78

Table 2 (continued)

m in mg	θ in °C	Partial thermal decomposition	Loss in %	
			Theor.	Exp.
Th(DMBP)$_4$ [a]				
0.233	30–115	$2H_2O$	3.16	3.13
3.188	165–360	$4(CH_3)_2$-N-⌬	42.13	42.23
1.765	360–372	Rest of the ligand with formation of $Th(CO_3)_2$	23.86	23.91
0.515	372–480	$2CO_2$, with formation of ThO_2	7.71	6.98
Th(DMBP)$_4$ [b]				
0.249	30–125	$2H_2O$	3.16	3.24
3.224	170–400	$4(CH_3)_2$-N-⌬	42.13	41.98
2.380	400–700	Rest of the ligand, with formation of ThO_2	31.57	30.99

[a] Platinum crucible. [b] Alumina crucible.

tion occurs with a large number of consecutive or simultaneous steps and through a more complex pathway than that observed from the TG curves.

In all the TG curves, the first mass loss is due to the dehydration, and the temperature range over which it occurs is dependent on the metal present. In the thermal decomposition of these compounds in both crucibles used, formation of the respective carbonate as intermediate occurs for the calcium, strontium and barium compounds; for the nickel and thorium compounds, the formation of the carbonate occurs only in the platinum crucible. For the iron compound, the intermediate $Fe_2O_2CO_3$ is formed only in the platinum crucible and for the lanthanum compound, the intermediate $La_2O(CO_3)_3$ is formed in both crucibles.

Calculations based on the mass losses observed in the TG curves of these compounds suggest the partial thermal decomposition taking place in each step. The mass losses and the corresponding temperature ranges for the partial thermal decompositions of all the compounds are shown in Table 2.

The DSC curves are shown in Fig. 3. These curves show endothermic and exothermic peaks or exotherms that all accord with the mass losses observed in the TG–DTG curves up to 600°C. The first endothermic peak for all the compounds is ascribed to the dehydration. The exothermic peaks or exotherms due to the thermal decomposition are characteristic of each compound.

These curves also show that the thermal decomposition of the anhydrous compounds occurs through a complex pathway which is in agreement with the information obtained from the DTG curves.

4. Conclusions

The X-ray powder patterns verified that the more soluble compounds tend towards a crystalline structure and the least soluble indicate an amorphous structure.

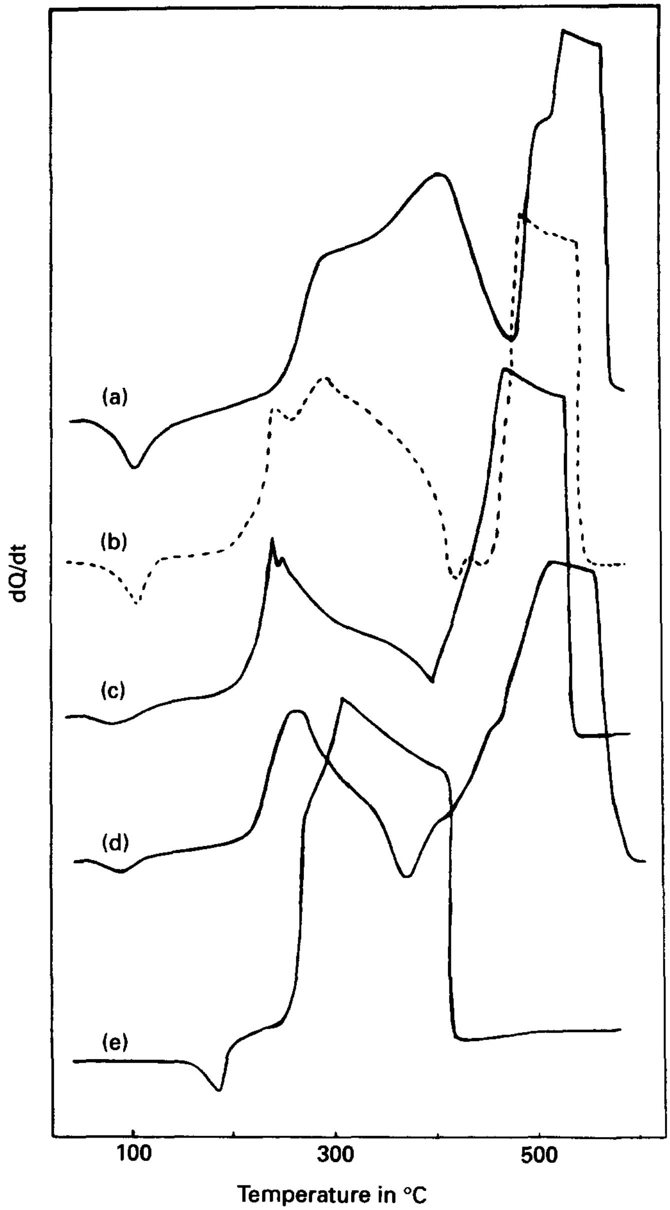

Fig. 3. DSC curves of (a) $Mg(DMBP)_2 \cdot 2H_2O$, (b) $Ca(DMBP)_2 \cdot 3.5H_2O$, (c) $Sr(DMBP)_2 \cdot 1.5H_2O$, (d) $Ba(DMBP)_2 \cdot H_2O$, (e) $Ni(DMBP)_2 \cdot 2.5H_2O$), (f) $Cu(DMBP)_2 \cdot 0.5H_2O$, (g) $Zn(DMBP)_2 \cdot H_2O$, (h) $Fe(DMBP)_3 \cdot H_2O$; (i) $La(DMBP)_3 \cdot 2H_2O$ and (j) $Th(DMBP)_4 \cdot 2H_2O$.

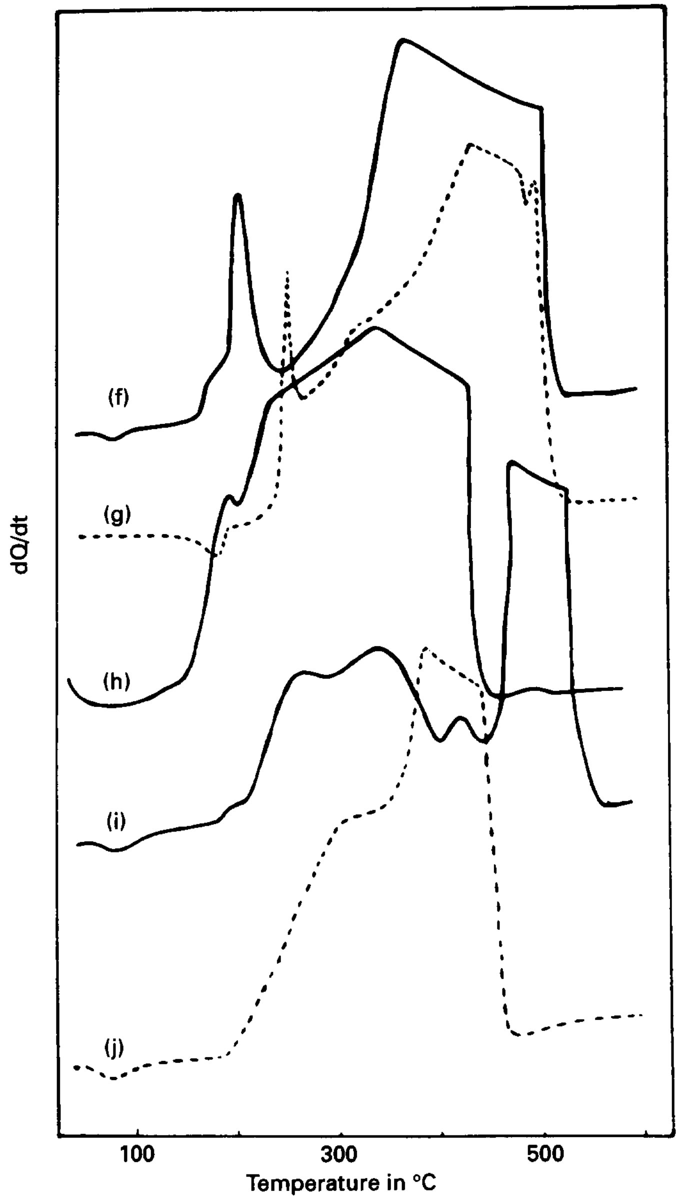

Fig. 3 (continued).

The TG–DTG curves established the stoichiometry of the compounds in the solid state and also provided information about the thermal stability and thermal decomposition.

Acknowledgments

The authors acknowledge the FAPESP (Proc. 90 2932-4) and CAPES for financial support.

References

[1] C.B. Melios, V.R. Torres, M.H.A. Mota, J.O. Tognolli and M. Molina, Analyst, 109 (1984) 385.
[2] C.B. Melios, J.T. Souza Campos, M.A.C. Mazzeu, L.L. Campos, M. Molina and J.O. Tognolli, Inorg. Chim. Acta, 139 (1987) 163.
[3] C.B. Melios, H. Redigolo and M. Molina, J. Inorg. Biochem. 36 (1989) 307.
[4] M.H. Miyano, C.B. Melios, C.A. Ribeiro, H. Redígolo and M. Ionashiro, Thermochim. Acta, 221 (1993) 52.
[5] H.A. Flaschka, EDTA Titrations, Pergamon, Oxford, 1964.
[6] C.N. de Oliveira, M. Ionashiro and C.A.F. Graner, Eclet. Quim., 10 (1985) 7.
[7] M. Ionashiro, C.A.F. Graner and J. Zuanon Netto, Eclet. Quim., 8 (1983) 29.
[8] J. Körbl and R. Pribil, Chemist-Analyst, 45 (1956) 102.
[9] L.C.S. de Oliveira, C.B. Melios, M. Spirandeli Crespi, C.A. Ribeiro and M. Ionashiro, Thermochim. Acta, 219 (1993) 215.
[10] M. Ionashiro, C.B. Melios, C.A. Ribeiro and M. Spirandeli Crespi, Thermochim. Acta, 168 (1990) 223.